On Modulation for Magnetic Induction based Transmission in Wireless Underground Sensor Networks

Steven Kisseleff
Institute for Digital Communications
Friedrich-Alexander-University (FAU)
Erlangen-Nürnberg, Germany
Email: kisseleff@lnt.de

Ian F. Akyildiz
Broadband Wireless Networking Lab
Georgia Institute of Technology
Atlanta, USA
Email: ian.akyildiz@ee.gatech.edu

Wolfgang Gerstacker
Institute for Digital Communications
Friedrich-Alexander-University (FAU)
Erlangen-Nürnberg, Germany
Email: gersta@lnt.de

Abstract—**Wireless underground sensor networks (WUSNs) are an emerging and promising research area. The aim of WUSNs is to establish an efficient wireless communication in the underground medium. A magnetic induction (MI)-based waveguide technique has been proposed to overcome the very harsh propagation conditions in WUSNs. In this approach, several resonant relay circuits are deployed between the two nodes to be connected. This technique allows for an extension of the transmission range. In this work, we investigate digital transmission schemes for MI-WUSNs. We analyze the influence of transmission parameters like symbol duration and modulation scheme and propose methods for their optimization.**

I. INTRODUCTION

Wireless underground sensor networks (WUSNs) are an emerging and promising research area. In WUSNs, the goal is to establish an efficient wireless communication in the underground medium. Typical applications for such networks include soil condition monitoring, earthquake prediction, border patrol, etc. [1], [2]. Since the propagation medium is soil, rock, and sand, traditional wireless signal propagation techniques using electromagnetic (EM) waves can be only applied for very small transmission ranges due to a high pathloss and vulnerability to changes of soil properties, such as moisture [3], [4].

Magnetic induction (MI)-based WUSNs were first introduced in [2], and make use of magnetic antennas implemented as coils, which are combined in waveguide structures with several passive relay devices between two transceiver nodes [5]. Similar to traditional wireless relaying concepts this approach is supposed to benefit from a lower pathloss. A distinct advantage of MI relays is that these devices do not need any power supply, such that the energy has to be provided only in the transceiver nodes, which can be recharged by removable or mobile aboveground devices [6].

In previous work, some efforts were made to characterize the channel conditions of MI-based transmission. Magneto-inductive waveguides with metamaterials were considered in [7], where the signal is described as an MI wave traveling through the channel. Based on this a corresponding noise model was proposed in [8]. In [5], [9], and [10] some channel

models for MI-WUSNs with frequency-selective pathloss were introduced. More realistic channel and noise models for a point-to-point transmission were derived in [11]. These models incorporate the losses due to the transmission medium and the power reflections between the coils. Furthermore, it was shown that a transmission through a conductive medium like soil can only be established using a carefully optimized set of system parameters. Based on this work, different sets of optimal parameters for MI waveguides with a high relay density in WUSNs were proposed in [12]. In [13], a set of system parameters was determined for direct MI transmission (without relays) for maximizing the throughput of WUSNs. The previous works mostly consider the channel capacity as performance measure. However, real methods of digital transmission for WUSNs have not been published yet.

In this work, for a fundamental insight in transceiver design for MI-WUSNs, we utilize the models from [11], which provide sufficient information about the channel characteristics. According to [11], due to the losses in the medium, MI waveguides with low relay densities are not applicable, because even for the optimal system parameters the resulting channel capacity of such links is below that of the direct MI transmission with no relays deployed. However, if the relay density is large, the coupling between coils is strong enough to cope with losses, resulting in an increased channel capacity. Therefore, we investigate two cases: direct MI transmission with no relays used and MI waveguides with a high relay density of $\frac{1 \text{ Relay}}{3 \text{ m}}$.

We address the following issues. For the two cases described above, we determine the most efficient transmission bandwidth, which corresponds to the symbol duration. We analyze the performance of the MI based transmission by means of the signal-to-noise ratio per transmitted data symbol in order to determine the optimal modulation scheme, which is still an open issue for underground communication [2]. For each type of transmission channel, we show an approach to minimize the data rate losses due to modulation schemes with finite alphabet size. Furthermore, we investigate how a modulation scheme should be chosen according to the performance requirements and in case of environmental changes. This provides a background for future transceiver design and system adaptation.

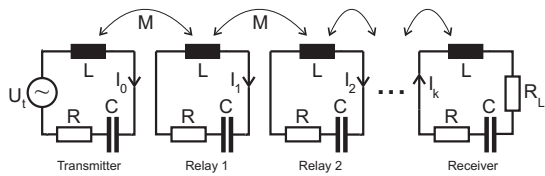In order to enable a coded transmission, a proper coding

Fig. 1.   MI waveguide with equidistant relay devices.

scheme has to be chosen. For WUSNs, the encoder and decoder design differs from the designs for traditional cellular systems, since the complexity of both transmitter and receiver should be low from the perspective of the energy consumption. Hence, the choice of the code can be seen as an optimization problem with practical constraints like target error rate, code rate, and complexity. This issue requires further exhaustive investigations, which are beyond the scope of this work. Therefore, we focus on modulation schemes and filter design for uncoded transmission, which should provide a good basis for the future development of coded transmission for WUSNs. This paper is organized as follows. In Section II the system model is presented and the signal processing components within the MI transceiver are specified. In Section III modulation and equalization for MI based transmission are addressed and the key solutions are given. Section IV provides simulation results and Section V concludes the paper.

II. System Modeling

Similar to [5], we assume that the waveguide structure contains one transmitter circuit with a voltage source U_t, one receiver circuit with a load resistor R_L, and $(k-1)$ passive relays, which are placed equidistantly between the transceivers, see Fig. 1. If no relays are deployed, the transmitter induces the voltage in the receiver circuit directly. Each circuit includes a magnetic antenna (which in this work is realized by a multilayer air core coil), a capacitor C, and a resistor R (which models the copper resistance of the coil and depends on the wire radius). We do not consider parasitic effects, such as skin effect in windings, proximity effect, and parasitic capacities, which may occur in circuit elements at very high frequencies. Instead, it is assumed that in the frequency band used for transmission the influence of these effects is negligible. Because all involved signal mappings are linear for MI based transmission, a linear channel model results. The capacitance of the capacitor is chosen to make each circuit resonant at frequency f_0 [5], i.e., $C = \frac{1}{(2\pi f_0)^2 L}$, where L denotes the inductivity of the coil. The induced voltage is related to the coupling between the coils, which is determined by the mutual inductance [14]

$$M = \mu \pi N^2 \frac{a^4}{4r^3} (2\sin\theta_t \sin\theta_r + \cos\theta_t \cos\theta_r) \cdot G, \quad (1)$$

where r denotes the distance between two adjacent coils, a stands for the coil radius, N is the number of windings, and μ denotes the permeability of the medium. θ_t and θ_r are the angles between the coil radial directions of transmitter and receiver, respectively, and the line connecting the two coil centers [13]. G is an additional loss factor due to eddy currents as pointed out in [11]. We assume that all devices are deployed in a homogeneous conductive environment (soil) with constant
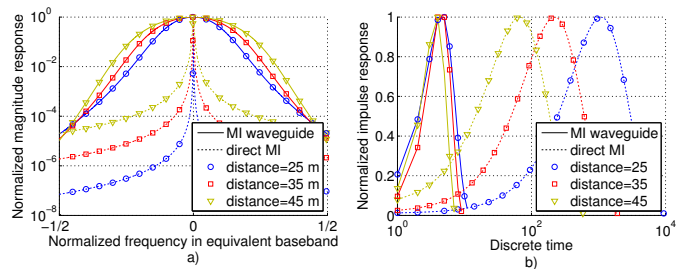

Fig. 2.   Examples for MI-based transmission channels: a) magnitude of frequency response; b) impulse response.

properties over space and time.

The resonant frequency f_0 and the number of windings N are chosen to maximize the achievable data rate with a given transmit waveform according to [11].

A. Channel and noise

We utilize the channel model for MI waveguides proposed in [11] with a channel transfer function $H(f)$ according to

$$H(f) = \frac{U_r(f)}{U_t(f)} = \frac{I_k(f)R_L}{U_t(f)} = \frac{x_L}{S(x, x_L, k+1)}, \quad (2)$$

where $x = \frac{R + j2\pi f L + \frac{1}{j2\pi f C}}{j2\pi f M}$ and $x_L = \frac{R_L}{j2\pi f M}$. The function $S(x, x_L, n)$ was introduced in [11] and can be determined as follows:

$$S(x, x_L, n) = F(x, n) + x_L \cdot F(x, n-1), \quad (3)$$

$$F(x, n) = \frac{(\frac{(x+\sqrt{x^2-4})}{2})^{n+1} - (\frac{(x-\sqrt{x^2-4})}{2})^{n+1}}{\sqrt{x^2-4}}. \quad (4)$$

Some examples for the transfer functions for different waveguides are depicted in Fig. 2a)[1]. It seems not possible to give a closed-form solution for the corresponding impulse responses in time domain shown in Fig. 2b) which have been calculated by numerical inverse discrete Fourier transform.

The noise power density spectrum is obtained via summation of the contributions from the noise sources within the waveguide. Due to a strong coupling between the coils for the optimal choice of the system parameters, noise contributions of all sources need to be taken into account. In this work, we focus on the thermal noise, which occurs in the copper wire of the coils and at the load impedance in the receiver circuit. The receive noise power density spectrum is given by [11]

$$E\{P_{\text{noise}}(f)\} = E\{P_{N,R}(f)\} + E\{P_{N,R_L}(f)\}, \quad (5)$$

$$E\{P_{N,R}(f)\} = \frac{1}{2} \frac{4K_B T_K R R_L}{|j2\pi f M|^2} \quad (6)$$

$$\times \sum_{n=0}^{k} \left(|S(x, x_L, n)|^2 \left| \sum_{m=n}^{k} \frac{1}{S(x, x_L, m)S(x, x_L, m+1)} \right|^2 \right),$$

$$E\{P_{N,R_L}(f)\} = \frac{1}{2} \frac{4K_B T_K R_L^2}{|j2\pi f M|^2} \quad (7)$$

$$\times \left| \sum_{m=0}^{k} \frac{1}{S(x, x_L, m)S(x, x_L, m+1)} \right|^2,$$

[1]Here, the frequency in equivalent baseband has been normalized by $\frac{1}{T}$, where T is the symbol interval, which is independently optimized for each MI based transmission channel with regard to the achievable data rate.

where $K_B \approx 1.38 \cdot 10^{-23}$ J/K is the Boltzmann constant, $T_K = 290$ K is the temperature in Kelvin, and $\mathrm{E}\{\cdot\}$ denotes the expectation operator.

As it was shown in [11], the general optimization problem of maximizing the channel capacity of MI based transmission (both for direct MI transmission and MI waveguides) is non-convex. However, suboptimal solutions for direct MI transmission and MI waveguides based transmission were proposed in [13] and [12], respectively. We borrow the following equations for the optimum frequency f_0 from these works.

1) Direct MI transmission:

$$f_0 = \left(\frac{2}{r\sqrt{\pi \sigma \mu}} \right)^2, \qquad (8)$$

where σ denotes the conductivity of the soil. The number of coil windings N is set to the maximum value restricted only by the coil size.

2) MI waveguides:

$$f_0 = \frac{1}{2\pi \sqrt{L(N) C_0}}, \qquad (9)$$

where C_0 stands for the minimum allowed capacitance of the capacitor as pointed out in [11] and $L(N)$ indicates that the inductivity L depends on N. Here, a full search using the discrete variable N can be applied to maximize the channel capacity.

However, in a practical system, the channel capacity from [11], [14], or the network throughput from [12], [13], are not the proper measures for the achievable data rate. Specifically, the transmit pulse was usually assumed to comply with the water filling rule which maximizes the channel capacity [15]. Such pulses are not applicable in practice in general. Instead, a smooth band-limited waveform is used for pulse shaping. Given the transmit filter $A \cdot H_t(f)$ with the amplification coefficient A, the total consumed transmit power results from [11]

$$P_t = \frac{1}{2} \int_B \frac{|A \cdot H_t(f)|^2}{|j2\pi f M|} \frac{|S(x, x_L, k)|}{|S(x, x_L, k+1)|} \mathrm{d}f, \qquad (10)$$

where B is the bandwidth of the transmitted waveform. Factor A can be determined to fulfill a given transmit power constraint. The resulting achievable data rate can be determined using Shannon's capacity equation

$$R_{ad} = \int_B \log_2 \left(1 + \frac{|A \cdot H_t(f) \cdot H(f)|^2}{|\mathrm{E}\{P_{\mathrm{noise}}(f)\} \cdot (2R_L)|} \right) \mathrm{d}f, \qquad (11)$$

where $H(f)$ and $\mathrm{E}\{P_{\mathrm{noise}}(f)\}$ are defined in (2) and (5), respectively[2].

B. Filter Design

A realistic approach for the filter design utilizes a square-root Nyquist transmit filter like a root-raised cosine (RRC) filter, which however does not maximize the achievable data

---

[2] A part of the transmit power density spectrum, $\frac{|S(x, x_L, k)|}{|j2\pi f M| \cdot |S(x, x_L, k+1)|}$, is already included in $|H(f)|^2$, because the transmitter circuit is viewed as a part of the transmission channel in MI-based links.

rate. Though, the bandwidth of the filter is optimized in order to maximize the resulting data rate. For receive filtering we employ the whitened matched filter (WMF) [16]. Here, the overall channel becomes minimum-phase, and the noise after sampling is white. Since the total transmission channel is frequency-selective, an equalization scheme is needed for the signal detection. In order to avoid further losses in data rate, for our performance investigations we use a decision-feedback equalization (DFE) scheme, which minimizes the mean-squared error (MSE) of the output signal (MMSE-DFE). For coded transmission, MMSE-DFE equalization would need to be replaced by Tomlinson-Harashima-Precoding (THP) [17].

III. MODULATION AND CODING

In order to provide specific design rules, we give recommendations for selection of a modulation scheme and symbol rate. For a given target symbol error rate (SER_t), e.g. $\mathrm{SER}_t = 10^{-3}$, and a signal-to-noise ratio (SNR) at the output of the equalizer SNR_{eq}, the constellation size M of the modulation scheme for a maximum data rate under the given performance constraint can be determined using the equations from [18], e.g. for M-QAM modulation type

$$\mathrm{SER}_t \leq 4 \cdot Q \left(\sqrt{\frac{3 \cdot \mathrm{SNR}_{eq} K}{M - 1}} \right), \qquad (12)$$

where $Q(\cdot)$ is the complementary Gaussian error integral and K is the coding gain of the employed channel code. This leads to

$$\log_2 M = \left\lfloor \log_2 \left(1 + \frac{3 \cdot \mathrm{SNR}_{eq} K}{c} \right) \right\rfloor, \qquad (13)$$

where the constant c depends on the prescribed target error rate. The $\lfloor \cdot \rfloor$ operator is applied, because we restrict our constellation sizes to powers of two. The overall data rate equals $R_d = \frac{R_c \log_2 M}{T}$, where R_c is the code rate and T denotes the symbol interval. If realistic codes with finite lengths are applied in a practical system, the corresponding coding gain K at the target SER should be used for the calculation. The modulation scheme and the code itself should be chosen to maximize the overall data rate. In addition, the complexity of encoding and decoding is very crucial for the low-power sensor nodes and needs to be taken into account, as argued before. This issue is however beyond the scope of this work. Therefore, in the following, uncoded transmission with $K = 1$ and $R_c = 1$ is considered.

A. Modulation for MI based transmission

As mentioned before, we consider the direct MI transmission scheme and the MI waveguide with a high relay density in this work. There is a significant difference in the nature of the two approaches. For the direct MI transmission, the data rate is maximized, if the carrier frequency is low due to the frequency dependent eddy currents effect. For MI waveguides, the optimal carrier frequency is very high, because the coupling between adjacent coils is much stronger due to short distances between relay coils. In addition, the slopes of the channel transfer function are much steeper for MI waveguides than for the direct MI transmission. This is due to the fact, that every

additional relay attenuates the slopes of the channel spectrum further. Therefore, the optimal bandwidth for the direct MI transmission is larger than that for the MI waveguides. However, the region of low pathloss of the direct MI channel is very narrow, such that the channel impulse response is very long (up to several 10000 taps), see Fig. 2. Such channels cannot be equalized in a practical system. In particular, if MMSE-DFE is applied after the WMF, the feedback filter of DFE needs to have at least the length of the channel for a good performance. However, a filter with 10000 taps is not realistic.

As mentioned earlier, the optimal transmit bandwidth for the MI waveguide channels is very low, even if a high data rate is achievable. From this we deduce a very high SNR, which allows for a choice of a higher order modulation scheme. In addition, due to a transmission in a narrow band, the fluctuations within the band are very limited (see Fig. 2a)), such that the corresponding impulse response is short (below 10 taps). However, for many cases in waveguide transmission the SNR at the output of the equalizer is high enough to enable a modulation with 14-18 bit/symbol, which cannot be implemented. In these cases, even if a modulation order of 10 bit/symbol (which corresponds to 1024-QAM modulation[3]) is selected, the achievable data rate decreases by $\frac{10\text{bit}}{18\text{bit}} \approx 55\%$. We refer to this method as clipping.

B. Proposed solutions

1) Direct MI transmission: For the direct MI channels, the problems arising from long impulse responses can be solved by reducing the bandwidth. Hence, the width of the low pathloss band increases relatively to the symbol rate, thus reducing the number of channel taps. We choose the bandwidth (and therefore the symbol rate), for which the number of channel taps observed at the input of the equalizer is below 100. This strategy enables a practical realization of the equalizer filters and therefore of a practical system. We refer to this method as our default scheme. However, since not the whole bandwidth is utilized for transmission, losses of up to 95% of the achievable data rate are inevitable. Unfortunately, it is impossible to reduce these losses using conventional single-carrier transmission.

Alternatively, the total band can be split in parts, which are processed independently. This approach is similar to the traditional frequency-division multiplexing (FDM) approach with multiple sub-bands. Frequency-division is utilized in this context due to a very steep transition between the low pathloss band and the side bands. Here, three transmission bands are chosen, in order to keep the transceiver design as simple as possible, see Fig. 3. These bands are processed independently at the receiver using WMFs, which contain RRC filters as parts of the analogue matched filters. Hence, due to the frequency selectivity of the RRC filters, there is no power dissipation to the neighboring bands and no intercarrier interference (ICI). The width of the inner band (band 2) is determined according to the specified maximum length of the channel impulse

---

[3]Higher order modulation schemes beyond 1024-QAM are not considered in this work due to their high complexity, such that they are not applicable in the low-power sensor node transceivers.
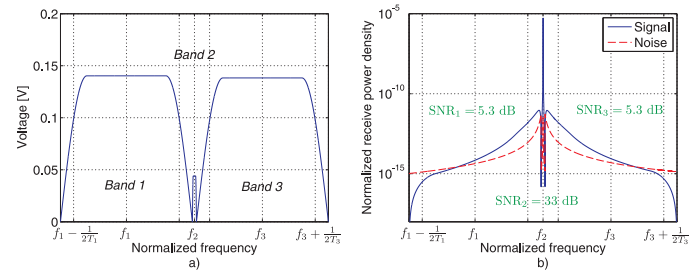

Fig. 3. Spectrum division for transmission distance $d = 22$ m. a) Transmit spectra in three frequency bands with center frequencies f_1, f_2, and f_3 using power allocation; the corresponding symbol intervals are T_1, T_2, and T_3; b) Received power density spectra (normalized to 1 W received power per sub-band) and SNR at the equalizer output.

response as described earlier. The other two bands (band 1 and band 3) occupy the remaining left and right parts of the spectrum, respectively. Due to a larger pathloss at the edges of the spectrum than at the resonance frequency, the SNRs for band 1 and band 3 may be very limited if equal power is allocated to all bands, such that no transmission is feasible in the side bands. On the contrary, due to a very low pathloss at the resonance frequency, the SNR for band 2 is very high, which enables a modulation with 10-12 bit/symbol. In order to provide a modulation of at least 1 bit/symbol (BPSK), the bands 2 and 3 need to be allocated more transmit power under the constraint $P_t = P_1 + P_2 + P_3$, where P_1-P_3 are the transmit powers in the corresponding transmission bands, respectively. Due to the small number of bands, the problem of finding the optimal power allocation can be solved by exploiting the symmetry of the bands. Then a full search in one variable, which corresponds to the power allocated to the inner band, can be performed.

With increasing number of sub-bands, the performance tends to approach the channel capacity because of the power allocation which approaches that of the water filling rule. Similarly, an orthogonal FDM (OFDM) scheme can be applied, which is beneficial for a large number of subcarriers. However, in order to decouple the OFDM blocks and to enable cyclic convolution for a practical implementation of OFDM, a guard interval has to be chosen at least as long as the channel impulse response, which has a length of over 10000 taps. Even if an appropriate channel shortening filter (with at most 100 taps) is applied, the resulting impulse response is very long, yielding a degradation of the data rate. Therefore, the practicality and efficiency of OFDM for the direct MI transmission in WUSNs still remains to be verified.

2) MI waveguides: As mentioned earlier, the bandwidth of the MI waveguides based channels is very limited. In order to reduce the loss of the clipping strategy, the bandwidth is chosen larger than the optimal bandwidth, which maximizes the data rate with unlimited constellation size. Hence, the SNR decreases and SER becomes worse, because less power is allocated to the frequencies with low pathloss and also the received noise power increases. This disadvantage is partially compensated for by the increased bandwidth/symbol rate. In fact, we convert the benefit of a large SNR into the benefit of a large bandwidth. We increase the bandwidth until the SER
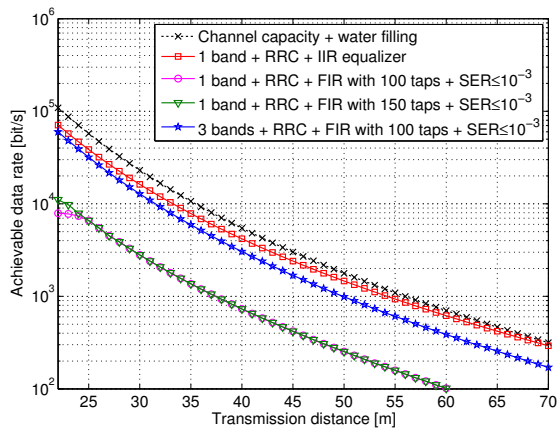
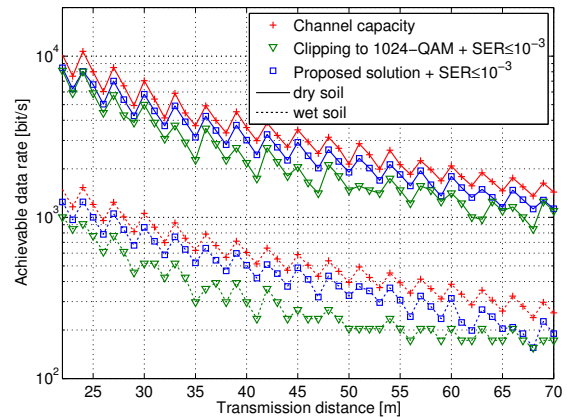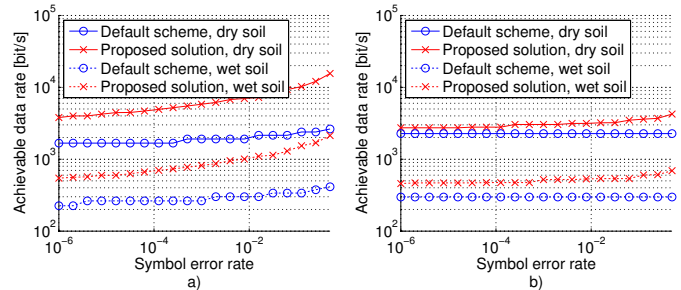Fig. 4.   Achievable data rate for direct MI transmission.

Fig. 5.   Achievable data rate for MI waveguides.

Fig. 6.   Achievable data rates for transmission distance $d = 35$ m with different target symbol error rates using a) direct MI transmission, b) MI waveguides.

fulfills the target SER constraint with equality for the chosen modulation scheme. A further increase in bandwidth (along with a reduction of M) may lead to longer impulse responses with more than 100 taps and is therefore not considered in this work.

IV. NUMERICAL RESULTS

In this section, we discuss numerical results for achievable data rates and the modulation order. In our simulations, we assume a total transmit power of $P_t = 10$ mW. We utilize coils with wire radius 0.5 mm and coil radius $a = 0.15$ m. The maximal number of coil windings N is 1000. The conductivity and permittivity of soil are $\sigma = 0.01$ S/m and $\epsilon = 7\epsilon_0$ for dry soil and $\sigma = 0.077$ S/m and $\epsilon = 29\epsilon_0$ for wet soil, respectively, where $\epsilon_0 \approx 8.854 \cdot 10^{-12}$ F/m. Since the permeability of soil is close to that of air, we use $\mu = \mu_0$ with the magnetic constant $\mu_0 = 4\pi \cdot 10^{-7}$ H/m. For a reduced pathloss, $\theta_t = \theta_r = \pi/2$ is assumed. The target SER is selected to $\mathrm{SER}_t = 10^{-3}$, and the roll-off factor of the used RRC transmit filter is 0.25.

First, we show results on the achievable data rate for direct MI transmission. Our observations on the modulation and filtering for transmission in wet soil are very similar to those in dry soil. Hence, we restrict ourselves to the direct MI transmission in dry soil. According to Fig. 4, large losses in achievable data rate are observed, if a finite impulse response (FIR) equalizer is used compared to the theoretical upper bound for uncoded transmission using an infinite impulse response (IIR) equalizer. Results for FIR filters of length 100 and 150 are depicted. A significant difference between the achievable data rates of these two cases appears only for low transmission distances, where the length of the channel impulse response is very large, see Fig. 2b). However, with increasing length of the equalizer filters, the data rate increases very slowly, such that several 10000 filter taps are needed to increase the data rate from ≈ 8 kbit/s for 22 m transmission distance to ≈ 71 kbit/s. We conclude that the big gap between the data rate of a practical system and the theoretical bound cannot be diminished, if a single-band transmission technique is applied. The proposed solution of utilizing three transmission bands with power allocation performs much better and achieves up to 85% of the theoretical limit of the uncoded single-band trans-

mission. For comparison, we also show the channel capacity for error free coded transmission, which has a negligibly small deviation from the channel capacity for coded transmission with $\mathrm{SER} = 10^{-3}$ [19]. Hence, it provides an upper bound for the data rate at the given SER. The proposed solution performs $\approx 45\%$ worse than the channel capacity, leaving a noticeable gap for the code design.

For MI waveguides, we compare the data rates of the proposed solution of bandwidth expansion with that of clipping for dry and wet soil, respectively, see Fig. 5. The proposed solution outperforms the clipping approach and performs slightly worse compared to the channel capacity. In addition, we observe that the proposed solution with increased bandwidth is even more beneficial for deployment in a wet soil environment than in dry soil, where the gain compared to the clipping approach is limited to 82%. This is due to the reduced bandwidth for transmission in wet soil compared to transmission in dry soil. Hence, the power is more concentrated in a very narrow frequency region, such that a larger SNR results and correspondingly a larger constellation is needed.

For a given transmission distance of $d = 35$ m, we investigate the achievable data rates with different target SER requirements, see Fig. 6. Here, "default scheme" refers to transmission within the inner band and the clipping method for direct MI transmission and MI waveguides, respectively. We observe that the data rate can be substantially improved by the proposed schemes, especially for a high target SER. This motivates the use of coded transmission. With decreasing target SER, the
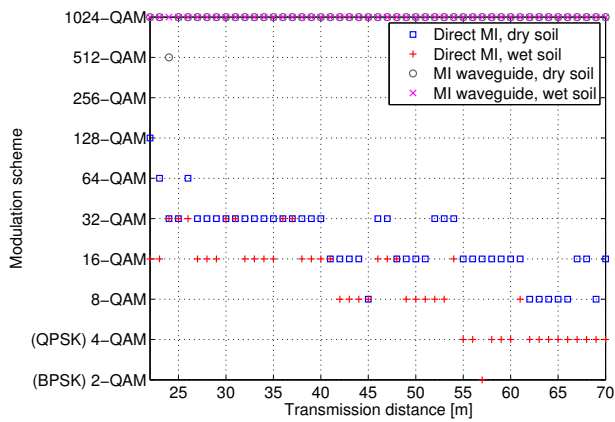
Fig. 7.   Proposed modulation schemes.

data rate for all transmission schemes reduces, except for the clipping scheme for MI waveguides, because the SNR at the equalizer output is still above the threshold SNR for a lower modulation order. In addition, we observe a staircase decrease of the achievable data rate for the remaining schemes, except for the proposed solution for direct MI transmission. This is due to the power allocation in the latter scheme, which introduces an additional degree of freedom, thus improving the data rate and smoothing the curve.

Finally, we present the modulation schemes, which should be chosen for an uncoded transmission in order to guarantee the target SER under the given assumptions, see Fig. 7. For the direct MI transmission, the modulation scheme for the inner frequency band is given only, because the side bands are modulated with BPSK symbols in most of the cases as described before, except for very high error rate, i.e., $\mathrm{SER}_t > 10^{-2}$, or for relatively short transmission distances, i.e., $d \le 45$ m. For the MI waveguides, the optimal constellation is mostly 1024-QAM, which corresponds to the clipping bound. For direct MI transmission, the pathloss in the inner band is much larger in wet soil medium than in dry soil. Hence, the modulation order in wet soil is lower or equal to the modulation order in dry soil. In addition, we observe a large variety of modulation schemes for direct MI transmission, varying between BPSK and 128-QAM. Furthermore, the modulation order for a transmission in the inner band descreases non-monotonically due to the varying widths of the side bands for different transmission distances and due to the power allocation. In a larger network with several transmission links, a unification of the transmission and system parameters is needed for a feasible manufacturing. Therefore, an optimal modulation scheme for a set of transmitting devices should be chosen based on the network topology and from the perspective of the network throughput optimization [12], [13]. This investigation is, however, beyond the scope of this work.

V. Conclusion

In this paper we considered the design of MI transceivers for uncoded transmission in WUSNs. For the two most relevant cases (direct MI transmission and MI waveguides), we provided the maximum achievable data rates, which can be ob-

tained in a point-to-point transmission using realistic transmit, receive, and equalization filters. In addition, recommendations for the symbol duration and modulation scheme have been given, which maximize the achievable data rate for a specified symbol error rate. Furthermore, for direct MI transmission, the problem of equalizing a very long channel impulse response is circumvented by utilizing a frequency-division based scheme with three transmission bands. For MI waveguides, a very high modulation order can be avoided using a bandwidth expansion approach. A significant increase in data rate is observed compared to the default transmission schemes.

References

[1] I.F. Akyildiz, W. Su, Y. Sankarasubramaniam, and E. Cayirci, "Wireless sensor networks: A survey," *Comput. Netw. J.*, vol. 38, pp. 393–422, March 2002.

[2] I.F. Akyildiz and E.P. Stuntebeck, "Wireless underground sensor networks: Research challenges," *Ad Hoc Netw. J.*, vol. 4, pp. 669–686, July 2006.

[3] I.F. Akyildiz, Z. Sun, and M.C. Vuran, "Signal propagation techniques for wireless underground communication networks," *Physical Communication Journal (Elsevier)*, vol. 2, pp. 167– 183, September 2009.

[4] L. Li, M.C. Vuran, and I.F. Akyildiz, "Characteristics of underground channel for wireless underground sensor networks," in *Proc. IFIP Mediterranean Ad Hoc Networking Workshop 2007*, June 2007.

[5] Z. Sun and I.F. Akyildiz, "Magnetic induction communications for wireless underground sensor networks," *IEEE Trans. on Antennas and Propag.*, vol. 58, pp. 2426–2435, July 2010.

[6] A. Karalis, J.D. Joannopoulos, and M. Soljacic, "Efficient wireless non-radiative mid-range energy transfer," *Annals of Physics*, vol. 323, pp. 34– 48, January 2008.

[7] R.R.A. Syms, I.R. Young, and L. Solymar, "Low-loss magneto-inductive waveguides," *Journal of Physics D: Applied Physics*, vol. 39, pp. 3945–3951, September 2006.

[8] R.R.A. Syms and L. Solymar, "Noise in metamaterials," *Journal of Applied Physics*, vol. 109, no. 124909, June 2011.

[9] H. Jiang and Y. Wang, "Capacity performance of an inductively coupled near field communication system," in *Proc. of IEEE International Symposium of Antenna and Propagation Society*, July 2008.

[10] J.I. Agbinya and M. Mashipour, "Power equations and capacity performance of magnetic induction communication systems," *Wireless Personal Communications Journal*, vol. 64, no. 4, pp. 831–845, 2012.

[11] S. Kisseleff, W.H. Gerstacker, R. Schober, Z. Sun, and I.F. Akyildiz, "Channel capacity of magnetic induction based wireless underground sensor networks under practical constraints," in *Proc. of IEEE WCNC 2013*, April 2013.

[12] S. Kisseleff, W. Gerstacker, Z. Sun, and I.F. Akyildiz, "On the throughput of wireless underground sensor networks using magneto-inductive waveguides," in *Proc. of IEEE Globecom 2013*, December 2013.

[13] S. Kisseleff, I.F. Akyildiz, and W. Gerstacker, "Interference Polarization in Magnetic Induction based Wireless Underground Sensor Networks," in *Proc. of IEEE PIMRC 2013 – International Workshop on Wireless Sensor Networks Standardization and Applications*, September 2013.

[14] Z. Sun and I.F. Akyildiz, "On capacity of magnetic induction-based wireless underground sensor networks," in *Proc. of IEEE INFOCOM 2012*, March 2012, pp. 370–378.

[15] D. Tse and P. Viswanath, *Fundamentals of Wireless Communication*. Cambridge University Press, 2005.

[16] J.G. Proakis, *Digital Communications*. McGraw-Hill Higher Education, 2001.

[17] G.D. Forney and G. Ungerboeck, "Modulation and Coding for Linear Gaussian Channels," *IEEE Trans. on Information Theory*, vol. 44, no. 6, pp. 2384–2415, October 1998.

[18] A. Goldsmith, *Wireless Communications*. Cambridge University Press, 2005.

[19] J.P. Aldis, "Capacity of digital communication system with allowed nonzero error rate," *Electronic Letters*, vol. 28, no. 13, pp. 1252–1253, June 1992.